Synthesis of Silver Nanoparticle-Immobilized Antibacterial Anion Exchange Membranes for Salinity Gradient Energy Production by Reverse Electrodialysis*

Mine Eti[1], Aydın Cihanoğlu[1], Kadriye Özlem Hamaloğlu[2], Esra Altıok[1], Enver Güler[3*], Ali Tuncel[2], Nalan Kabay[1*]

[1]Department of Chemical Engineering, Ege University, İzmir, 35100, Türkiye

[2]Department of Chemical Engineering, Hacettepe University, Ankara, 06800, Türkiye

[3]Department of Chemical Engineering, Atılım University, Ankara, 06830, Türkiye

ABSTRACT

Biofouling, stemming from the attachment of living microorganisms, such as bacteria, which form resilient biofilms on membrane surfaces, presents a significant challenge that hampers the efficiency of anion exchange membranes (AEMs) in reverse electrodialysis (RED) applications. This limitation curtails the generation of electrical power from salinity gradients, which, notably, is a sustainable form of energy known as osmotic energy. Reverse electrodialysis (RED) stands as a clean and promising process to harness this sustainable energy source. This study aimed to impart antibacterial activity to the synthesized AEMs using silver nanoparticles (AgNPs). For that purpose, AgNPs were synthesized at 30^{o}C using two different pH (6.0 and pH 9.0) and immobilized into synthesized AEMs using the dip-coating technique. In nanoparticle synthesis, ascorbic acid (AA) and trisodium citrate (TSC) were used as a reductant and a stabilizer, respectively, to take under control of particle size and agglomeration behavior. The results indicated that AgNPs synthesized at pH 6.0 were dispersed on the AEMs surface without agglomeration. The stability of AgNPs immobilized on the membrane surface was tested under low and high-saline solutions. The antibacterial activities of AEMs were determined with the colony-counting method using Gram-negative (*Escherichia coli*) bacteria

Published by ACS Sustainable Chemistry and Engineering,
https://doi.org/10.1021/acssuschemeng.3c06320

suspension. The viability of bacteria dramatically decreased after the immobilization of AgNPs to the AEMs. In the short and long-term RED tests, it has been observed that the AEMs having AgNPs have high energy-generating potentials, and power density up to 0.372 W/m^2 can be obtained.

Keywords: Biofouling, Anion exchange membranes, Reverse electrodialysis, Silver nanoparticles, Antibacterial activity.

Corresponding authors:

N.Kabay (nalan.kabay@ege.edu.tr) & E.Güler (enver.guler@atilim.edu.tr)

Published by ACS Sustainable Chemistry and Engineering,
https://doi.org/10.1021/acssuschemeng.3c06320

1. INTRODUCTION

Fouling of ion exchange membranes (IEMs) is one of the most important constraints of the RED process.[1] The source and type of the feed solution have a significant impact on membrane fouling because of the wide range of pollutants present in different feed solutions. Colloidal (clays, flocs), organic (oils, polyelectrolytes, humic and fulvic acid), scaling (mineral), biological (bacteria, fungi) are the most prevalent forms of pollutants for membranes. Cation exchange membranes (CEMs) in the RED system are more prone to scaling because of their structural and electrochemical characteristics, while AEMs have less resistance to organic and biological fouling.[2] It is reported in the literature that energy harvesting performance by the RED system was dramatically decreased due to the presence of biological and organic fouling in the feed water.[3-5] Even though pretreatment of feed water is an alternative for eliminating foulant, imparting antifouling behavior to IEMs is an inevitable fact. It is possible to construct highly selective AEMs without increasing the membrane's electro-resistance to prevent fouling. Various surface modification techniques can be used for this purpose. These modifications can be categorized as solution casting,[6] graft polymerization,[7] dip coating/immersion,[8] electrodeposition,[9] layer-by-layer deposition,[10,11] plasma treatments.[12] Of the modification techniques listed, dip coating /immersion is the most suitable for surface coating because it is simple, low-cost, additional chemicals free, and highly repeatable.

Silver is the most effective nanoparticle against viruses, bacteria, and other eukaryotic organisms due to their small size, high surface area, and ability to bind to matrices.[13,14] In addition to its antibacterial capabilities, covering AEMs with AgNPs improved its selective and ionic permeability,[15] ionic conductivity,[13] thermal stability,[16] and values compared to the unmodified membrane. In the study of Vaselbehagh et al., they looked at AEMs biofouling during RED tests and tried to modify their surfaces to make them less susceptible to

Published by ACS Sustainable Chemistry and Engineering,
https://doi.org/10.1021/acssuschemeng.3c06320

biofouling.[17] Radzig et al. reported on antibacterial action of AgNPs on gram-negative bacteria along with mechanism of action, influence on the growth and biofilms formation.[18]

Nanocomposite AEMs for RED applications have not been prepared specifically yet. A restricted number of nanoparticles and polymeric materials have been employed to prepare the IEMs specific to the RED system. In the majority of RED research, commercial AEMs were utilized. Some studies were performed by coating their surface with a polyelectrolyte solution to create an antifouling membrane for RED systems, decreasing the membranes' ionic resistance and increasing their selective permeability.[17,19,20] In this work, for the first time, antibacterial AgNPs immobilized AEMs were synthesized for salinity gradient energy production by RED, and their characterizations were done.

2. MATERIAL AND METHODS

The AEMs were prepared from a polymer solution by casting method followed by the solvent evaporation. For the synthesis of membranes, poly(epichlorohydrin), PECH (37 wt% chlorine, Osaka Soda Co., Ltd), as the active polymer and poly(acrylonitrile), PAN (Mitsubishi Chemical Co. Ltd.), as the inert polymer were used. To provide a good mechanical stability to the membranes, the crosslinker, 1,4-diazabicyclo[2.2.2]octane, DABCO (Reagent Plus≥99%, Sigma- Aldrich) with diamine functionality was used. For the synthesis of silver nanoparticles (AgNPs), silver nitrate ($AgNO_3$), ascorbic acid ($C_6H_8O_6$), trisodium citrate ($Na_3C_6H_5O_7$), citric acid ($H_3C_6H_5O_7$), sodium hydroxide ($C_6H_8O_6$), obtained from Sigma-Aldrich Co. were employed. The membrane synthesis details were given previously.[21] The membranes used in the study and their properties are given in Table 1.

Published by ACS Sustainable Chemistry and Engineering,
https://doi.org/10.1021/acssuschemeng.3c06320

Table 1. Properties of the membranes.

Membranes	ER-BR	SD (%)	IEC (mmol/g dry membrane)	FCD (mmol/g H_2O)
ER4-BR1.07	4-1.07	66.28	3.47	5.24
ER2-BR0.6	2-0.6	25.56	1.47	5.70

ER: Excess diamine ratio, BR: Blend ratio, SD: Swelling degree, IEC: Ion exchange capacity, FCD: Fixed charge density. SD, IEC, FCD calculations were given previously.[21]

2.1. Synthesis of AgNPs

AgNPs were synthesized in a water bath at a constant temperature of 30°C using ascorbic acid (AA) as a reductant and trisodium citrate (TSC) as a stabilizer with solution pH of 6.0 and 9.0. An 8.0 mL aqueous solution containing AA (6.0×10^{-4} M) and TSC (3.0×10^{-3} M) was adjusted to different pH value (6.0 and 9.0) by addition of 0.2 M citric acid or 0.1 M NaOH solution. A 0.08 mL of 0.1 M of $AgNO_3$ solution was added under a stirring speed of 900 rpm at 30°C in water bath. After 15 min, no further change in color (blue) took place, indicating the reaction was completed.[22]

2.2. AgNPs immobilized AEMs

Immobilization of the synthesized AgNPs to the anion exchange membranes synthesized was carried out in an acidic environment to observe the behavior of membranes in an acidic environment. To this end, two different ways were followed. In the first way, the pH of the AgNPs solution was adjusted to an acidic environment (pH 2.0), and then the membranes were added to this environment. In the second way, first, the membranes were added to the AgNPs solution, and then the pH of the nanoparticle solution in which the membranes were submerged was adjusted to 2.0. The relevant membrane samples names and conditions are given in Table 2. The AgNPs solution immobilization time was adjusted for 24 h.

Published by ACS Sustainable Chemistry and Engineering,
https://doi.org/10.1021/acssuschemeng.3c06320

Table 2. Immobilization of the synthesized AgNPs to AEMs.

Samples	Conditions
ER4-BR1.07	Diamine ratio: 4; Blend ratio: 1.07
1 (pH 6.0) 2 (pH 9.0)	ER4-BR1.07 membranes were washed with distilled water for 24 h and then immersed in AgNPs solution.
3 (pH 6.0-1)* 4 (pH 9.0-1)*	The pH of the AgNPs solution was adjusted to pH 2.0 first with the help of H_2SO_4, and then the washed membranes were added to the medium.
5 (pH 6.0-2)** 6 (pH 9.0-2)**	The washed membranes were immersed in the AgNPs solution first, then the pH of the medium was adjusted to 2.0 with the help of H_2SO_4.

* represents the 1st way and ** represents the 2nd way

2.3. Stability studies

The stability of AgNPs on the membrane surface was checked under two different saline water conditions. To this end, the AgNPs immobilized AEMs were exposed to 0.017 M and 0.5 M NaCl solutions for 1 and 6 h, respectively. An inductively coupled plasma mass spectrometer (Perkin Elmer DRC II model ICP-MS) was used for the measurement of silver ions released during the stability tests. The AgNPs attached membranes (5 mg) were dissolved in HNO_3. Then, centrifugation (5000 rpm, 5 min) was made to remove membranes that could not be dissolved. Subsequently, 1 ml of sample was taken from supernatant and ICP-MS analysis was made. Thus, the values obtained from ICP-MS analysis indicated the silver contents of the membranes. With the calculations made from these values, the percentages of silver released from the membranes in stability tests were calculated.

2.4. Characterizations

The particle sizes of AgNPs were measured with Malvern Zeta sizer device. The UV-vis absorption spectra were obtained with a Thermoscientific Genesys 20 UV-vis

Published by ACS Sustainable Chemistry and Engineering,
https://doi.org/10.1021/acssuschemeng.3c06320

spectrophotometer. The chemical structure of membranes was determined by Fourier Transform Infrared Spectroscopy (FTIR, Perkin Elmer Spektrum 100) analysis. Thermo Scientific Apreo S model Scanning Electron Microscope (SEM) and Energy Dispersive X-Ray (EDX) mapping, Thermo Scientific K-Alpha model X-ray Photoelectron Spectroscopy (XPS), were utilized for structure analyses of the membranes, determining the particle loading amount and homogeneity on the membrane surface. Ion exchange capacity, swelling degree, and fixed charge density analysis details were calculated as reported before.[21]

2.4. Antibacterial activity of AEMs

The antibacterial activities of the bare and AgNPs immobilized AEMs were determined using the model gram-negative bacteria (*E. coli*) suspension with the colony counting method according to the ASTM E2149 standard protocol. First, *E. coli* was inoculated in Mueller-Hinton agar. Then, the bacteria were incubated at 37°C. After incubation, bacteria colonies were picked off with a swab and mixed with 0.1% (w) peptone water to adjust concentration to the value of 0.5 McFarland (2.5×10^7 CFU/mL) standards scale. Next, bacteria suspension was diluted with nutrient broth (the dilution ratio is 1:9 bacteria suspension: nutrient broth) to adjust the concentration to 2.5×10^6 CFU/mL and this was used as a stock suspension for the antibacterial tests. Before the antibacterial tests, membrane coupons (effective size: 3 cm x 3 cm) were first sterilized using a UV light for 30 min (each side was exposed to UV light for 15 min). Then, 100 µL of the stock bacteria suspension was added into a 250 mL of erlenmeyer flask containing 50 mL of phosphate buffered saline (PBS) solution.

Next, the membrane coupons were immersed in the bacteria suspension in the erlenmeyer flask and shaken at 200 rpm for 24 h at 37ºC. Finally, bacteria suspension was spread on the LB (Luria-Bertani) broth plates with 10^{-2} and 10^{-4} dilution rates, incubated for 24 h at 37ºC and the colonies were counted. In antibacterial activity calculation, inoculum solution (without

Published by ACS Sustainable Chemistry and Engineering,
https://doi.org/10.1021/acssuschemeng.3c06320

containing any membrane) was used as control. The antibacterial activity test was repeated three times (n=3). The bactericidal rate was calculated using Equation 1.[23]

$$Antibacterial\ rate, \%\ \left(\frac{CFU}{mL}\right) = \frac{N_P - N_M}{N_P} * 100 \qquad \text{Equation 1}$$

Where N_P and N_M are the number of visual bacteria colonies on the agar plate after contacting with the bare and AgNPs modified membranes, respectively.

2.5. RED Studies

In the RED studies, unmodified PECH-C membranes (ER2-BR0.6) and AgNPs immobilized PECH-C membranes (ER2-BR0.6) were used as AEMs together with NEOSEPTA CMX membranes used as CEMs. Properties of NEOSEPTA CMX are given in Table 3. Operating conditions of RED test are summarized in Table 4.

Table 3. Properties of NEOSEPTA CMX membranes.

Ion exchange capacity (mmol/g)	1.64±0.01
Area resistance ($\Omega.cm^2$)	3.43±0.16
Permselectivity (%)	92.5±0.6
Swelling degree (%)	21.5±0.2
Thickness (μm)	181±2.0

Table 4. Operating conditions of RED test.

Flow rates of feed solutions (mL/min)	30, 75, 120
Flow rate of electrode solution (mL/min)	300
Concentration of the feed solutions (g/L)	Dilute NaCl solution: 1 Concentrated NaCl solution: 30
Electrode solution	0.25M NaCl; 0.05M $K_3Fe(CN)_6$ 0.05M $K_4Fe(CN)_6$
AEMs and CEMs	ER2-BR0.6 and NEOSEPTA CMX
Salt ratio (g NaCl/L less saline solution:g NaCl/L high saline solution)	1:30
Number of membrane pair	3

Published by ACS Sustainable Chemistry and Engineering,
https://doi.org/10.1021/acssuschemeng.3c06320

3. Results and Discussion

3.1. Characterization of AgNPs and Immobilized AEMs

The particle size distributions of the AgNPs synthesized at pH 6.0 and pH 9.0 are given in Figure 1. The average particle size of AgNPs at pH 6.0 was 107.4 nm and that of pH 9.0 was 96.92 nm. Qin et al. determined the AgNPs produced at pH 6.0 and pH 9.0 as 89 nm and 62 nm, respectively,[22] while Steinigeweg and Schlücker determined the sizes of hemispherical as 83.9 nm±26.2%.[24] The sizes of the AgNPs synthesized in this study are consistent with the results given in the literature.

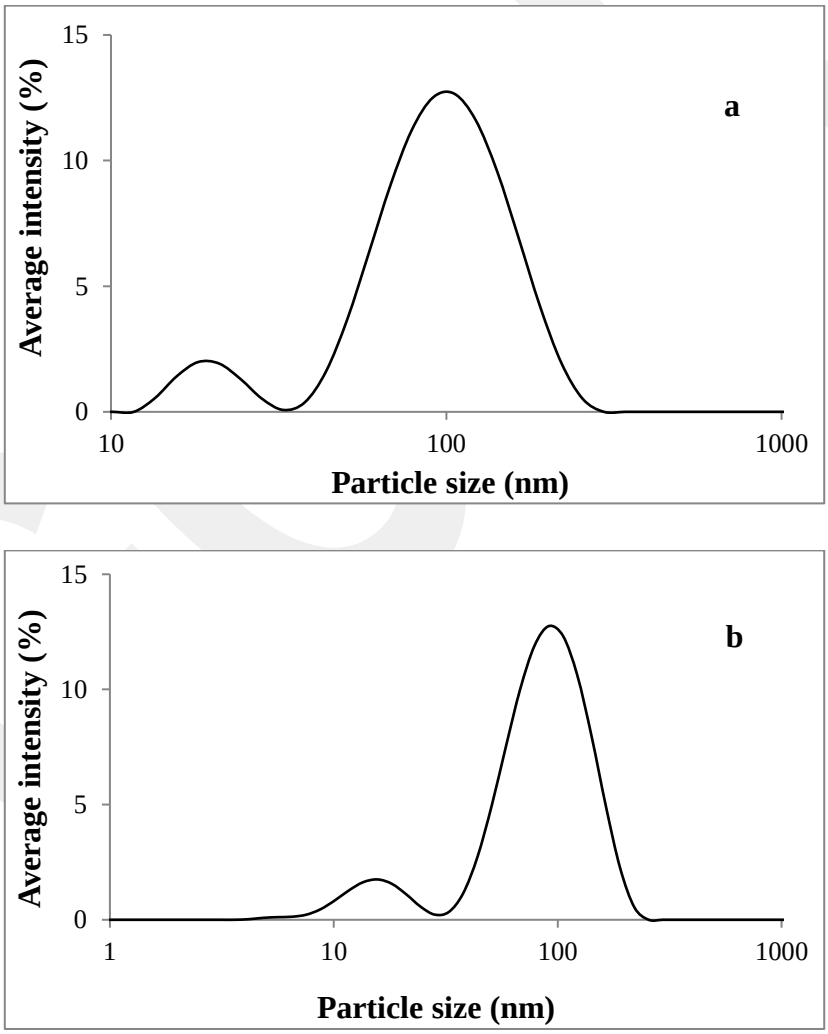

Figure 1. Size distribution of AgNPs produced at a) pH 6.0, b) pH 9.0.

Published by ACS Sustainable Chemistry and Engineering,
https://doi.org/10.1021/acssuschemeng.3c06320

The UV-vis absorption spectra of AgNPs prepared at pH 6.0 and pH 9.0 are given in Figure 2. The wavelengths related to the maximum absorbance were measured as 432 nm and 442 nm for AgNPs prepared at pH 9.0 and pH 6.0, respectively. Qin et al. obtained the wavelengths of AgNPs produced at pH 6.0 and pH 9.0 as 480 nm and 433 nm, respectively. In the other studies, wavelength of AgNPs were found as in the range of 402 to 462 nm.[25-28] In the literature, it was reported that sodium borohydride was used as primary reductant and trisodium citrate as secondary reductant as well as stabilizing agent.

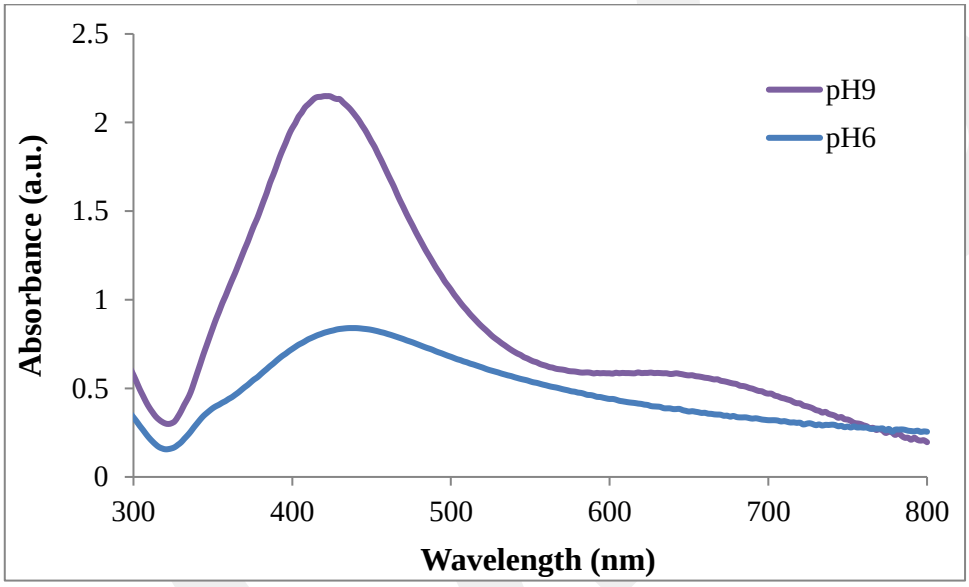

Figure 2. UV-vis spectra of AgNPs prepared at pH 6.0 and pH 9.0.

It was predicted that the negatively charged AgNPs would be better immobilized to the membranes by electrostatic interaction of the membranes with protonated amine groups in an acidic environment. The FTIR analysis was performed to understand whether there is degradation in the membrane structure in an acidic environment. The analysis results showed that no change was observed in the wavenumbers showing -C≡N and C-N bonds in the FTIR spectra of membranes immersed in acidic environment (pH 2) (Figure 3). Since no degradation was observed in the membranes in an acidic environment, AgNPs were produced and immobilization on the membranes in an acidic environment was carried out by dipping method.

Published by ACS Sustainable Chemistry and Engineering,
https://doi.org/10.1021/acssuschemeng.3c06320

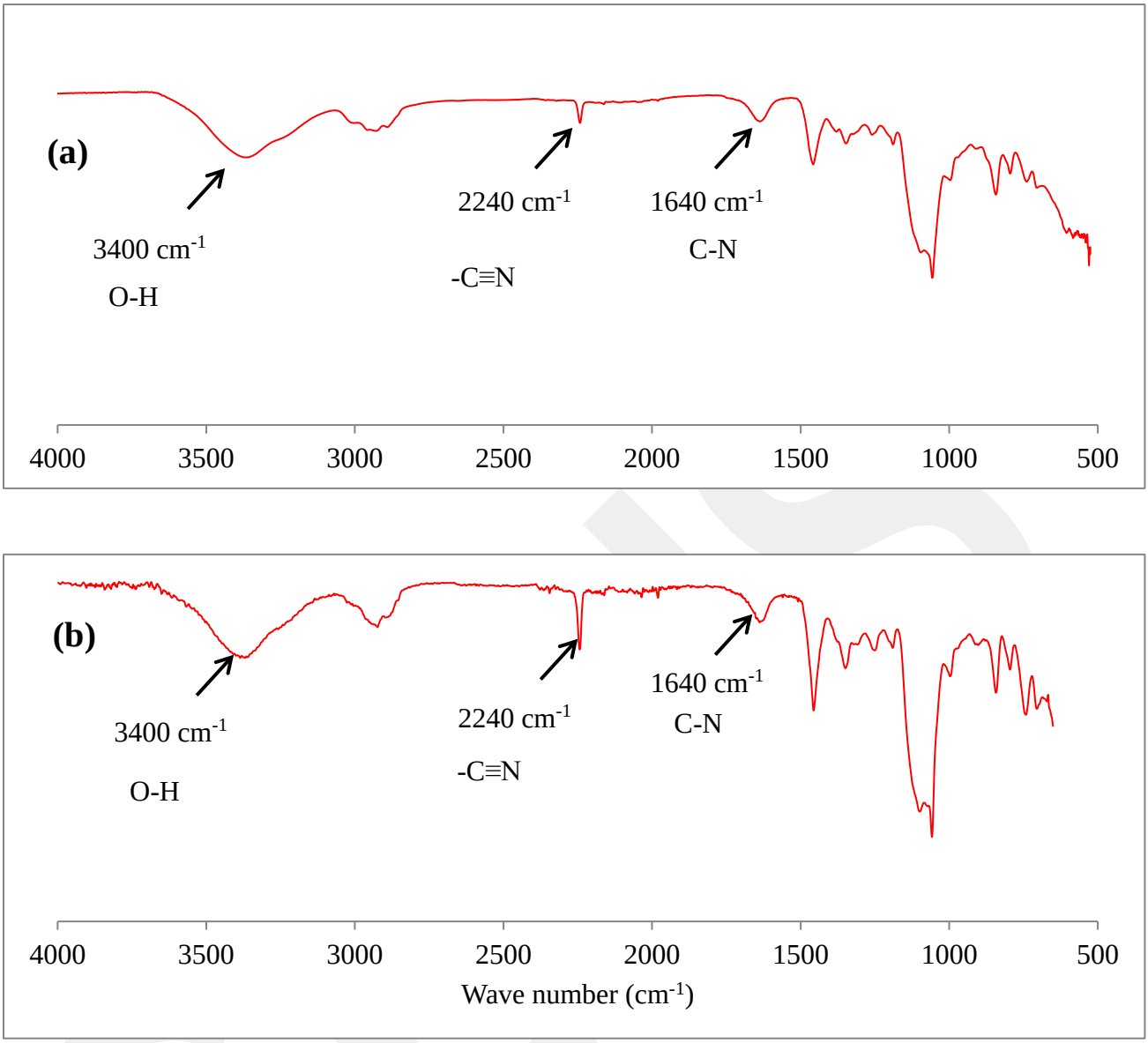

Figure 3. FTIR results of membranes immersed in (a) acidic and (b) neutral environment.

The SEM images of AEMs after nanoparticle immobilization are given in Figures 4 and 5. It is observed that there is an agglomeration in membranes after immobilization of AgNPs produced at pH 9.0. At high pH values, the rate of chemical reduction is high, and this caused the nanoparticles to aggregate. It is observed that the particle distribution is homogeneous after the immobilization of the AgNPs produced at pH 6.0 to the membrane without interacting with the acidic medium (pH 2.0) (Figures 4-b and 5-b). Agglomerations were formed at pH 9.0 medium (Figures 4-c and 5-c). When ascorbic acid is used as a reducing agent, the reduction reaction

Published by ACS Sustainable Chemistry and Engineering,
https://doi.org/10.1021/acssuschemeng.3c06320

occurs slowly at high pH and causes AgNPs to agglomerate and grow on the membrane surface. It was observed that the best dispersion was observed in membranes prepared at pH 6.0.

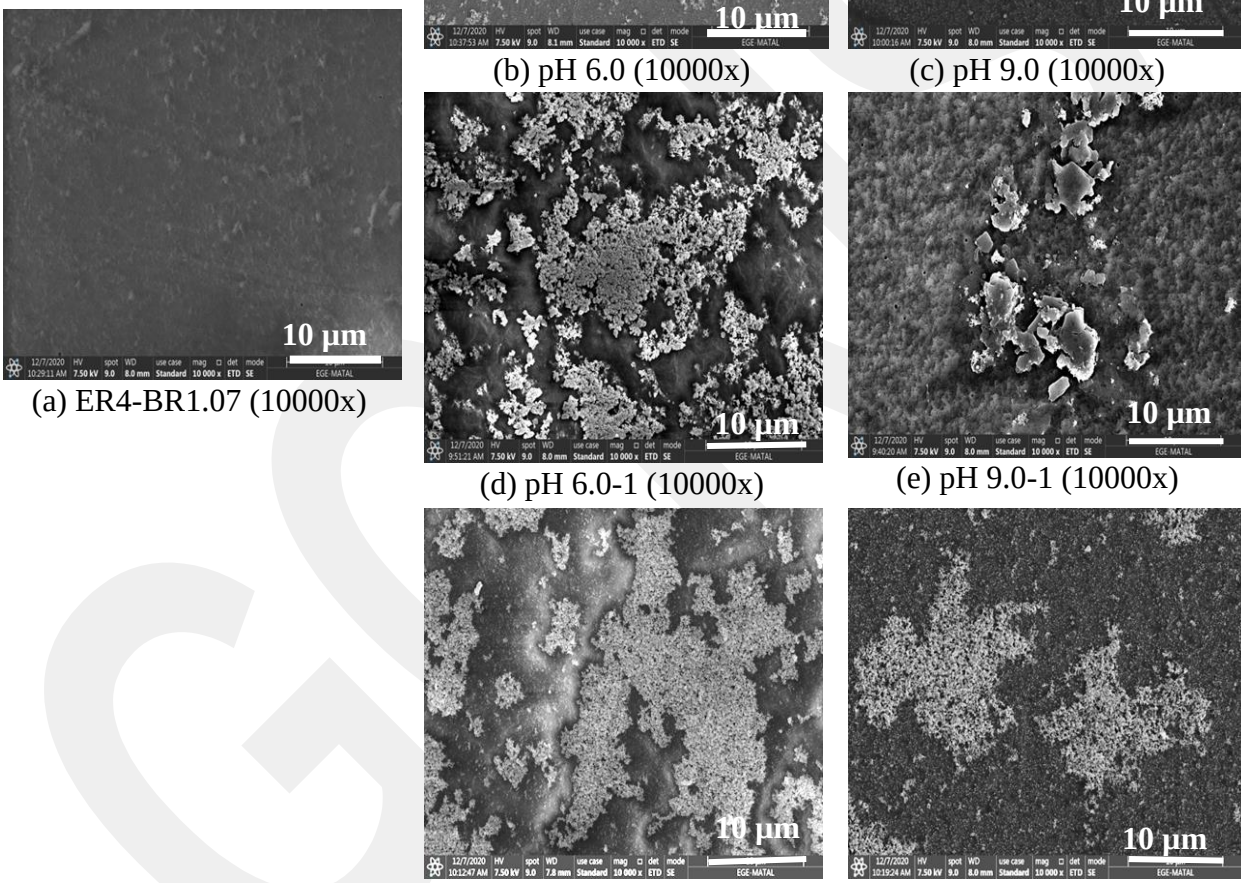

(a) ER4-BR1.07 (10000x)
(b) pH 6.0 (10000x)
(c) pH 9.0 (10000x)
(d) pH 6.0-1 (10000x)
(e) pH 9.0-1 (10000x)
(f) pH 6.0-2 (10000x)
(g) pH 9.0-2 (10000x)

Figure 4. SEM surface images after nanoparticle immobilization to membranes (10000x).

Published by ACS Sustainable Chemistry and Engineering,
https://doi.org/10.1021/acssuschemeng.3c06320

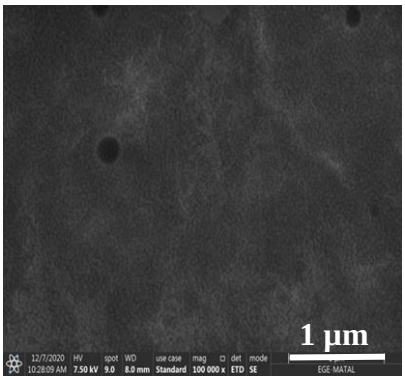

(a) ER4-BR1.07 (10000x)

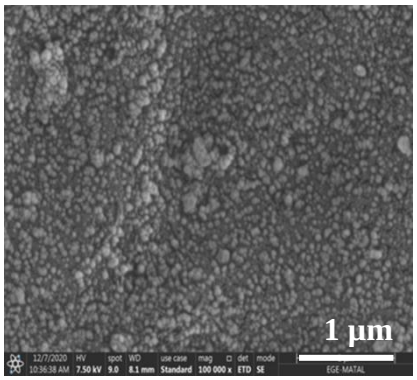

(b) pH 6.0 (100000x)

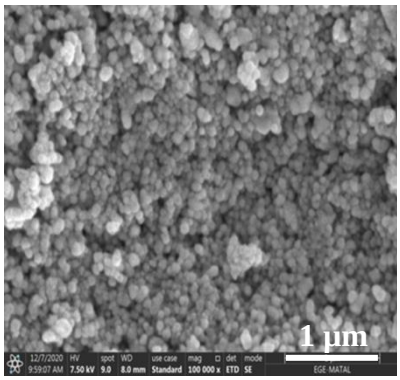

(c) pH 9.0 (100000x)

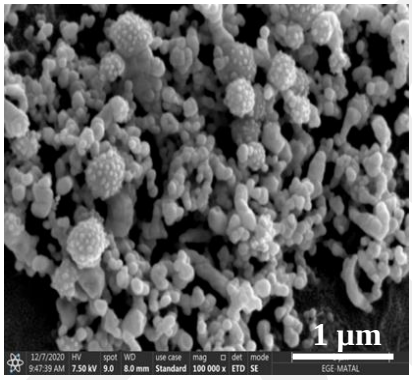

(d) pH 6.0-1 (100000x)

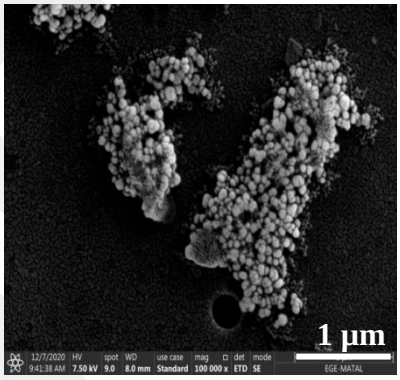

(d) pH 9.0-1 (100000x)

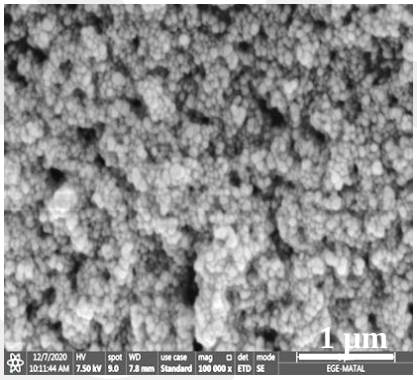

(e) pH 6.0-2 (100000x)

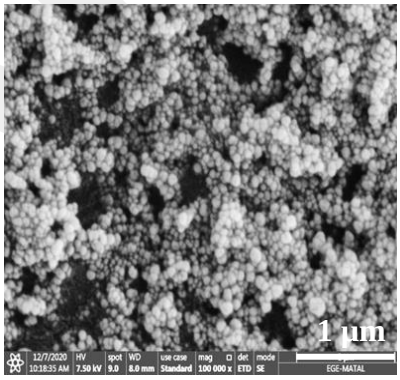

(f) pH 9.0-2 (100000x)

Figure 5. SEM surface images after nanoparticle immobilization to membranes (100000x).

Published by ACS Sustainable Chemistry and Engineering,
https://doi.org/10.1021/acssuschemeng.3c06320

The overall XPS spectrum for chemical components determination on the surface of AgNPs immobilized membranes (ER4-BR1.07) is given in Figure 6. It is seen that all the elements (O, Ag, N, C and Cl) expected to be on the membrane surface are detected. The O, C, N, and Cl elements are from the structure of the PECH-based AEM, and Ag is observed because of the AgNPs immobilized on the membrane surface.

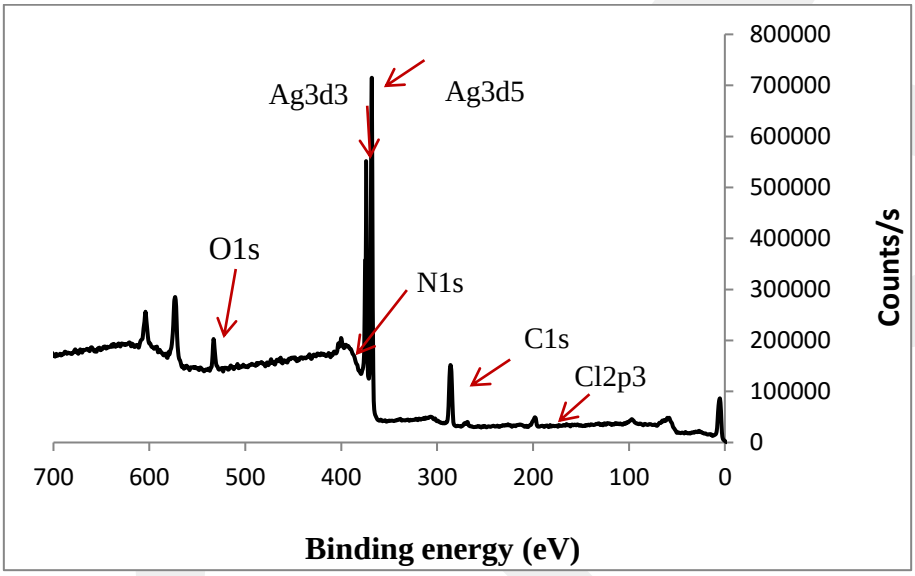

Figure 6. XPS Spectrum of AgNPs immobilized AEM.

When the Ag3d core level XPS spectrum given in Figure 7 is examined, specific Ag3d bands belonging to metallic Ag are seen at 368.4 eV and 374.4 eV. In addition, the absence of a specific 369.4 eV band belonging to Ag nanoclusters indicates that AgNPs are homogeneously immobilized on the membrane surface.

Published by ACS Sustainable Chemistry and Engineering,
https://doi.org/10.1021/acssuschemeng.3c06320

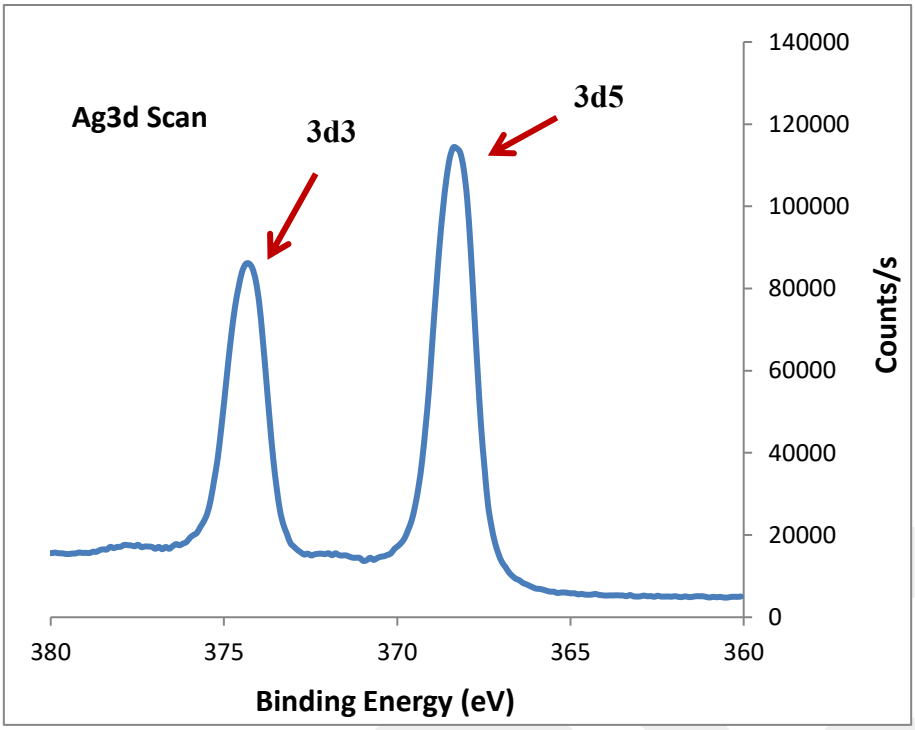

Figure 7. XPS spectrum of elements in the membrane structure.

3.2. Stability Test of AgNPs Immobilized AEMs

Stability tests were carried out to see and determine the release of AgNPs from the AgNPs immobilized AEMs when the AEMs are in contact with NaCl solutions at different concentrations and time. If the amount of AgNPs release is high, the resistance of AEMs to biofouling will decrease. It is aimed to keep the AgNPs release from AEMs as low as possible. The SEM images depicted in Figure 8 show the distribution of AgNPs on membrane surface. The SEM images of the AgNPs immobilized AEMs after contacted with 0.017 M and 0.5 M NaCl solutions for different periods are shown in Figures 9-12.

Published by ACS Sustainable Chemistry and Engineering,
https://doi.org/10.1021/acssuschemeng.3c06320

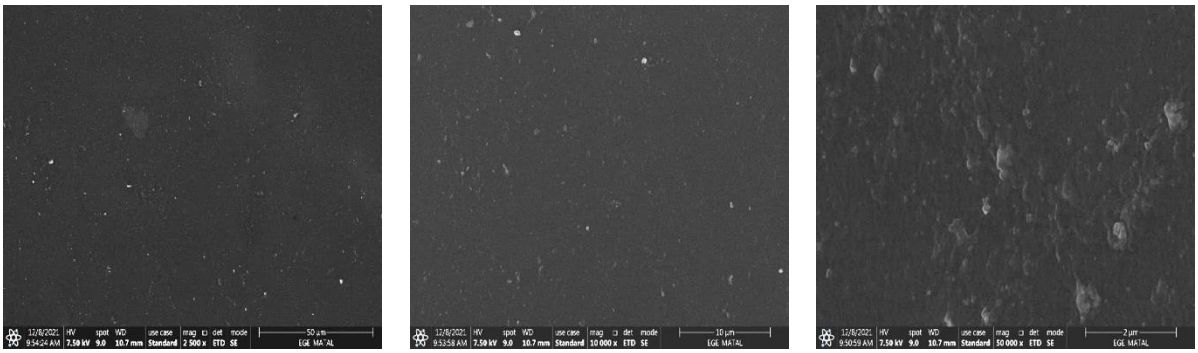

a **b** **c**

Figure 8. SEM surface images of the ER4-BR1.07 membrane before stability tests with the magnification of a) 2500x b)10000x c) 50000x.

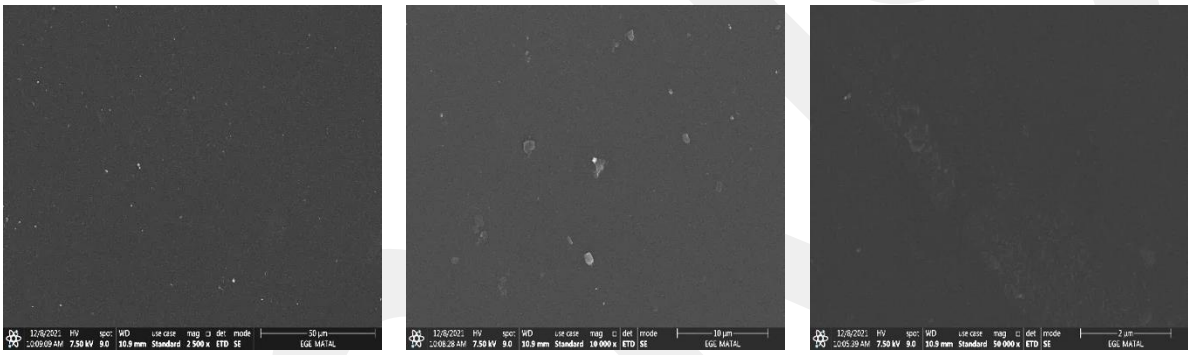

a **b** **c**

Figure 9. SEM surface images of the ER4-BR1.07 membrane after stability test in 0.017M NaCl at 1 h with the magnification of a) 2500x b)10000x c) 50000x.

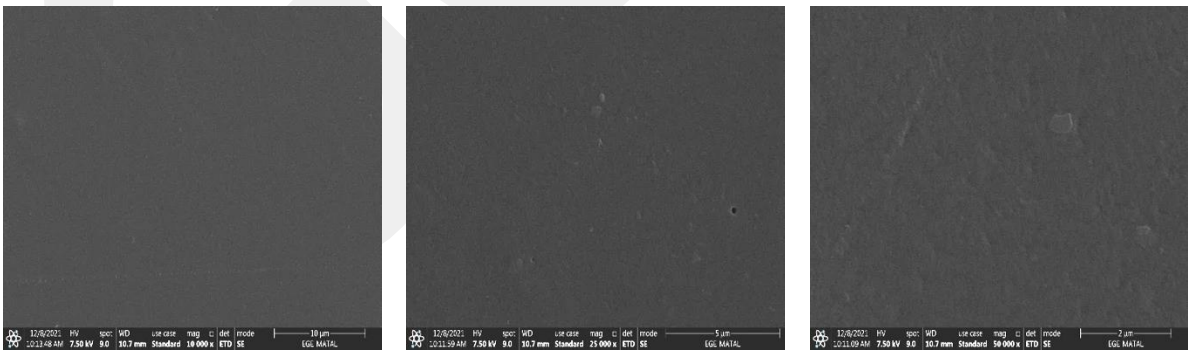

a **b** **c**

Figure 10. SEM surface images of the ER4-BR1.07 membrane after stability test in 0.017M NaCl at 6 h with the magnification of a) 2500x b) 25000x c) 50000x.

Published by ACS Sustainable Chemistry and Engineering,
https://doi.org/10.1021/acssuschemeng.3c06320

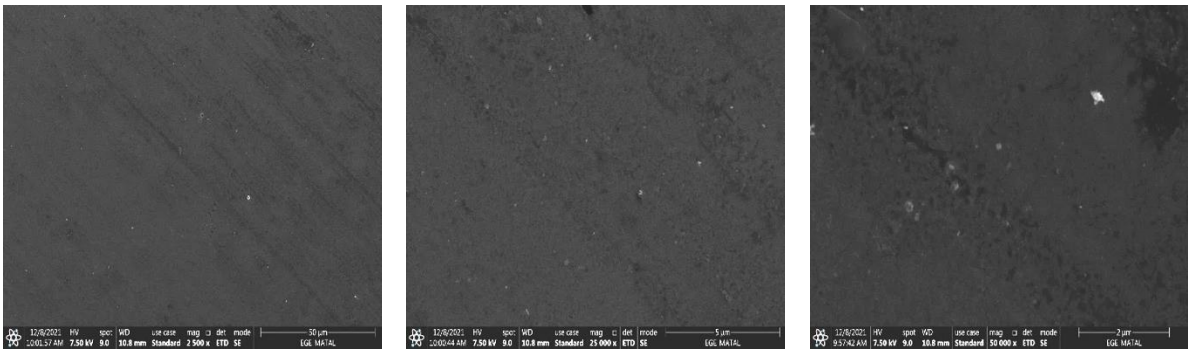

a **b** **c**

Figure 11. SEM surface images of the ER4-BR1.07 membrane after stability test in 0.5M NaCl at 1 h with the magnification of a) 2500x b) 25000x c) 50000x.

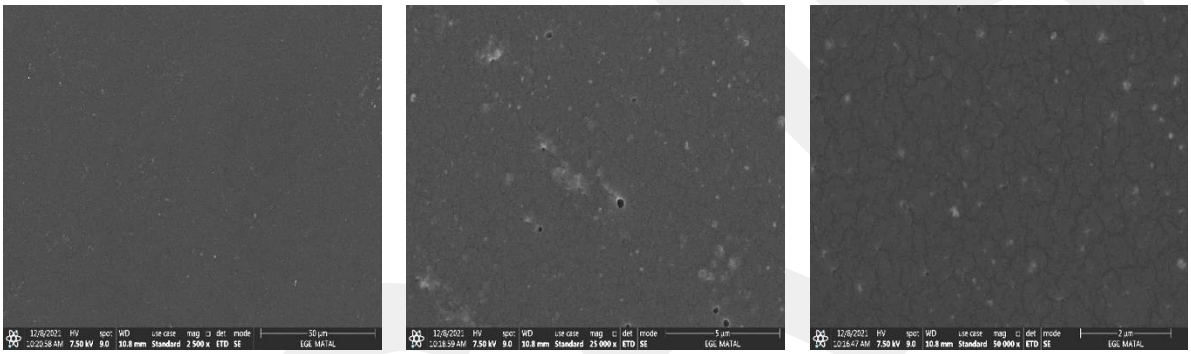

a **b** **c**

Figure 12. SEM surface images of the ER4-BR1.07 membrane after stability test in 0.5M NaCl at 6 h with the magnification of a) 2500x b) 25000x c) 50000x.

It was considered that the amount of AgNPs on the AEM seemed to decrease to some extent after contacted with NaCl solutions (Figures 9-12). However, there was no clear information from SEM images. Some information about release of AgNPs from the membrane surface is obtained from XPS analyses as well. The XPS analyses were carried out to see the atomic percentages of the AgNPs immobilized AEMs before and after exposure to NaCl solutions. The percentages of elements on the membrane surface immobilized AgNPs before and after stability test are given in Table 5. The amount of AgNPs on the membrane surface decreased by contacting membrane with especially 0.5 M NaCl solution. However, approximately the same

atomic percentage values were obtained after 1 h and 6 h of contacts with 0.017 M NaCl solution.

Table 5. Percentage of elements in AgNPs immobilized AEM by XPS analysis.

Contact condition with NaCl solution	S (%)	C (%)	Cl (%)	Ag (%)	N (%)	O (%)
No contact	0.32	82.62	0.47	0.15	4.18	11.82
0.017 M NaCl-1 h	0.18	67.83	1.92	0.17	9.14	20.76
0.017 M NaCl-6 h	0.77	72.68	2.91	0.18	8.83	14.63
0.5 M NaCl-1 h	0.23	74.20	2.82	0.06	7.83	14.86
0.5 M NaCl-6 h	0.85	74.60	2.16	0.05	8.98	13.37

In addition, the ICP-MS measurements were carried out to observe the AgNPs leakage from the membrane and to determine the amount of AgNPs immobilized on AEMs before and after the contact in NaCl solutions. The amount of Ag on the AEMs can be seen in Table 6. Maximum amount of Ag was observed for the membrane which is not contacted with NaCl solution. The amount of Ag decreased with increasing NaCl concentration in the contact solution.

Table 6. Amount of AgNPs immobilized on the AEMs.

Condition	Ag (µg/L) remained on the membrane
No contact with NaCl	185±9 (Loading amount)
0.017 M NaCl-1 h	74±5
0.017 M NaCl-6 h	42±3
0.5 M NaCl-1 h	11.2±0.8
0.5 M NaCl-6 h	16.8±0.8

3.3. Antibacterial Activity of AEMs

Figure 13 shows the antibacterial test results obtained with unmodified AEMs and AgNPs immobilized AEMs. Figure 13-a shows the results of control group which is the incubated medium without membrane, while Figures 13-b and c show the results of the AEMs and AgNPs

immobilized AEMs. Figure 14 indicates the quantification of bacteria viability. The results show that the bacteria viability was dramatically decreased after immobilization of AgNPs to the membrane surface. The unmodified AEMs had a 1 log reduction (antibacterial rate, 90%) observed in the viability of the bacteria, while a 5.5 log reduction (antibacterial rate, 99.999 %) was observed in the case of AgNPs immobilized AEMs. Similarly, in the study of Zhu et al. AgNPs was immobilized onto the surface of a chitosan membrane to examine the anti-biofouling performance of the membrane surface and bare membrane had a significantly higher bacteria coverage than the silver immobilized membranes.[29] Li et al. pointed to the possibility that AgNPs may alter the structure of bacterial cell membranes and reduce the activity of certain membranous enzymes, ultimately leading to the death of E. coli bacteria.[30] In the study of Vaselbehagh et al. the results demonstrated that AEM's anti-biofouling characteristics were enhanced by a polydopamine (PDA) layer during RED operation.[31] Yuksel et al. showed that the best antibacterial effects were seen in nanocomposite membranes that incorporated surface AgNPs storage.[32] In the study of Radzig et al. it has been observed that AgNPs can inhibit the growth of Gram-negative bacteria in both planktonic cells and biofilms.[33]

Published by ACS Sustainable Chemistry and Engineering,
https://doi.org/10.1021/acssuschemeng.3c06320

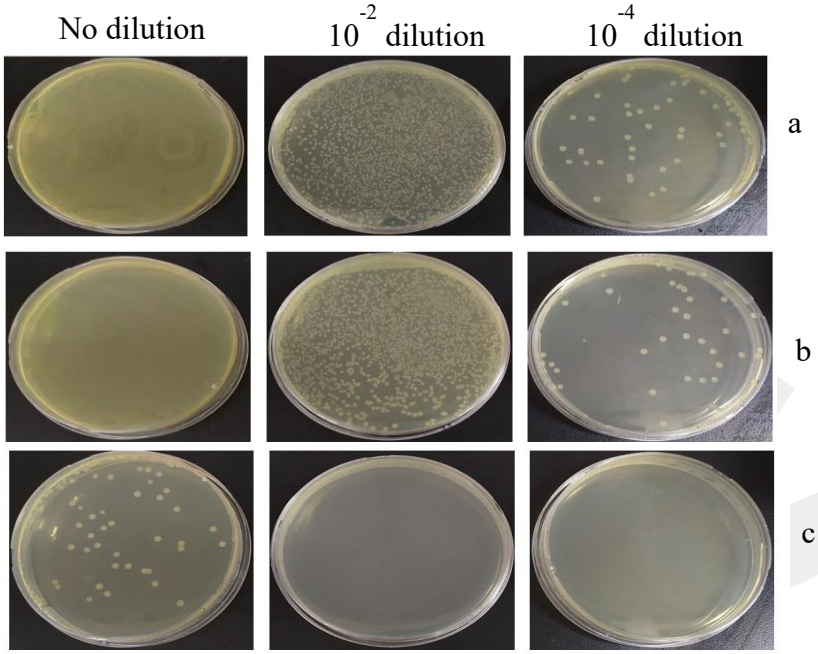

Figure 13. Results of the antibacterial tests a) Control (incubated medium without membrane), b) Unmodified AEMs, c) AgNPs immobilized AEMs.

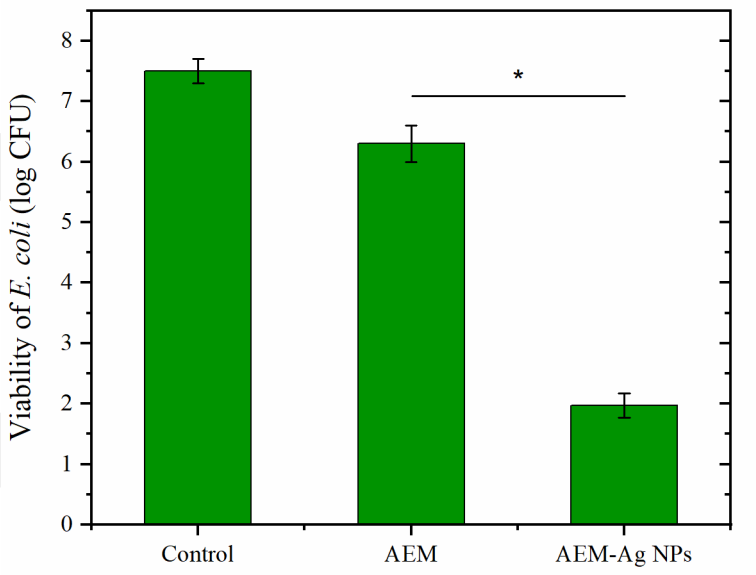

Figure 14. Antibacterial activity of the unmodified and AgNPs immobilized AEM against *E. coli* (Control; incubated medium without membrane) (* donates a p.≤0.05 significance between membranes).

Published by ACS Sustainable Chemistry and Engineering,
https://doi.org/10.1021/acssuschemeng.3c06320

3.4. RED Test Results

Karakoç and Güler found the highest power density produced by PECH-C (ER2-BR0.6) type membranes coupled with NEOSEPTA CMX was 0.32 W/m^2 and it was 0.39 W/m^2 for NEOSEPTA AMX and NEOSEPTA CMX.[34] In this study, AgNPs immobilized ER2-BR0.6 were used as AEMs, and NEOSEPTA CMX membranes as CEMs. At the same time, effect of feed flow rate was investigated. In RED test, flow rate of electrode solution was adjusted as 300 mL/min while flow rates of feed solutions were 30, 75 and 120 mL/min. The salt ratio was 1:30 (g NaCl/L less saline solution: g NaCl/L high saline solution) and the number of membrane pair was 3.

The power density vs. current density graphs obtained at different feed flow rates are depicted in Figure 15. Power density values increased with increasing flow rate and reached its highest value with 0.372 W/m^2.

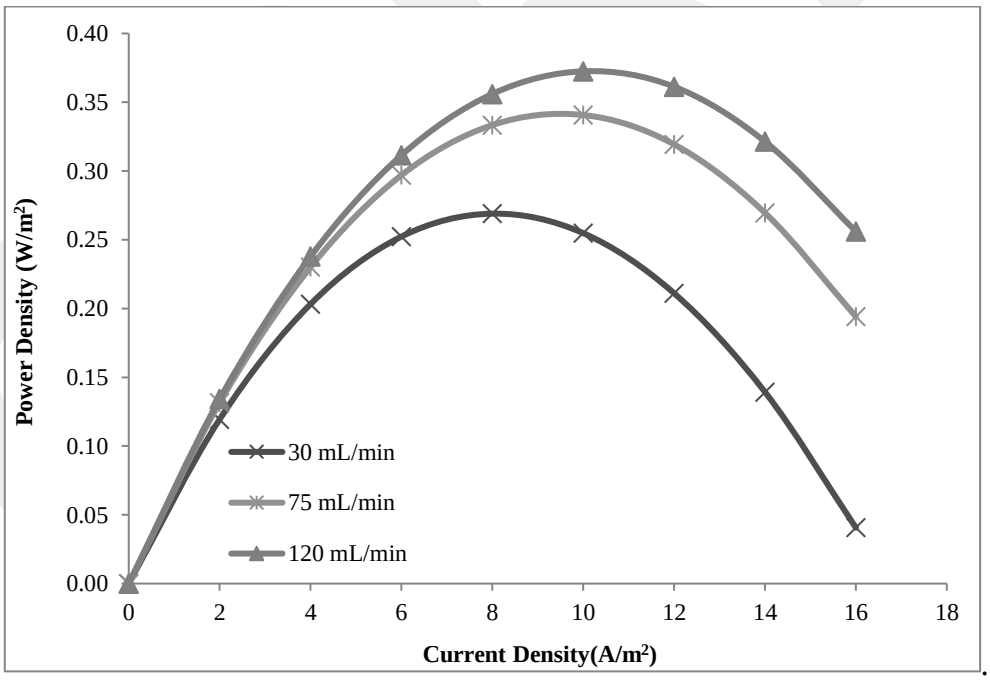

Figure 15. Power density vs. current density graph of short-term studies of AgNPs immobilized PECH-C membranes coupled with NEOSEPTA CMX.

Power density vs. time plot of the AgNPs immobilized PECH-C coupled with NEOSEPTA CMX during long term study is shown in Figure 16. The highest power density value obtained was 0.348 W/m^2 during long term study.

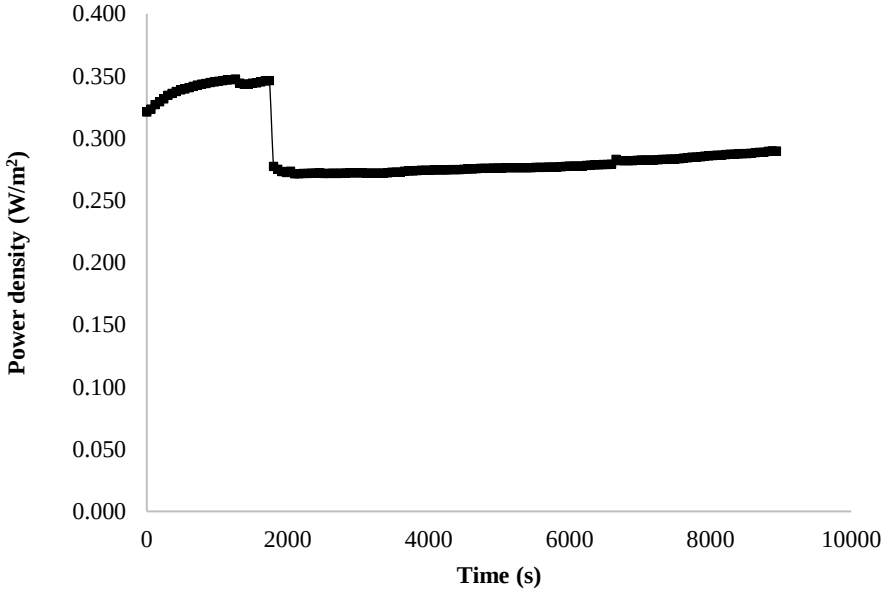

Figure 16. Power density vs. time plot for long-term studies of AgNPs immobilized PECH-C coupled with NEOSEPTA CMX.

The results obtained with short and long term RED studies are summarized in Tables 7 and 8. For PECH-C based AEMs paired with NEOSEPTA CMX and PECH-C membranes immobilized with AgNPs, the maximum power density values are 0.316 W/m^2 with 30 mL/min of feed flow rate and 0.372 W/m^2 with 120 mL/min of feed flow rate. For the AgNPs immobilized PECH-C AEMs, open circuit voltage values increased with increasing flow rate. On the other hand, with PECH-C based AEMs, open circuit voltage values decreased with increasing flow rate and fixed after 60 mL/min of feed flow rate. At 120 mL/min of feed flow rate, maximum power density value is higher with AgNPs immobilized PECH-C membranes. During long-term RED studies, maximum power densities of 0.222 W/m^2 and 0.348 W/m^2 were obtained for PECH-C membranes coupled with NEOSEPTA CMX and PECH-C membranes

Published by ACS Sustainable Chemistry and Engineering,
https://doi.org/10.1021/acssuschemeng.3c06320

immobilized with AgNPs, respectively. Highest power density is obtained as 0.348 W/m^2 during long term studies at 30 mL/min flow rate if we compare long term and short term studies. The maximum power density values increased due to the increase in conductivity in the AgNPs immobilized membranes.

Table 7. Short-term studies of unmodified and AgNPs immobilized AEMs coupled with NEOSEPTA CMX.

Membranes	**Salt ratio (g NaCl/L: g NaCl/L)**	**Number of membrane pairs**	**Flow rate of feed solutions (mL/min)**	**Maximum power density (W/m^2)**	**Open circuit voltage (V)**
AgNPs immobilized AEMs & NEOSEPTA CMX	1:30	3	30	0.269	0.409
			75	0.341	0.442
			120	0.372	0.448
AEMs & NEOSEPTA CMX			30	0.316	0.424
			60	0.275	0.433
			90	0.269	0.433
			120	0.264	0.433

Table 8. Long-term studies of unmodified and AgNPs immobilized AEMs coupled with NEOSEPTA CMX.

Membranes	**Salt ratio (g NaCl/L: g NaCl/L)**	**Number of membrane pairs**	**Linear flow velocity of feed solutions (mL/min)**	**Maximum power density (W/m^2)**
AEMs & NEOSEPTA CMX	1	3	30	0.222
AgNPs immobilized AEMs & NEOSEPTA CMX				0.348

Published by ACS Sustainable Chemistry and Engineering,
https://doi.org/10.1021/acssuschemeng.3c06320

4. Conclusions

Novel AgNPs-immobilized PECH-based anion exchange membranes were developed for the first time, demonstrating their potential in harnessing sustainable salinity gradient energy through the clean process of RED. It was observed that the particle distribution is homogeneous after the immobilization of the AgNPs produced at pH 6.0 and agglomerations were formed at pH 9.0. Although the percentages of AgNPs released from AEMs were high according to chemical analysis by ICP-MS, their antibacterial activity was still sufficient. The XPS results showed that AgNPs were immobilized uniformly on the membrane surface. A highest power density produced with AgNPs immobilized PECH-C membranes coupled with NEOSEPTA CMX was 0.348 W/m^2.

5. Acknowledgement

This study was supported through EIG Concert-Japan (Project no. TÜBİTAK 118M804). Mine Eti, acknowledges the scholarships given by TÜBİTAK. The authors acknowledge Mitsubishi Chemical, Japan, especially Mr. Ando Kiyoto for getting PAN samples and Osaka Soda Co., Japan for PECH polymer. One of the authors, Aydın Cihanoğlu would like to thank the financial support of TÜBİTAK through the National Postdoc project (Project No: 118C549).

REFERENCES

(1) Post, J.W. Blue energy: Electricity production from salinity gradients by reverse electrodialysis. Wageningen University, PhD Thesis, **2009**.

(2) Mikhaylin, S.; Bazinet, L. Fouling on ion-exchange membranes: classification, characterization and strategies of prevention and control. *Adv. Colloid Interface Sci.* **2016**, *229*, 34-56.

(3) Santoro, S.; Tufa, R. A.; Avcı, A. H.; Fontananova, E.; Profio, G. D.; Curcio, E. Fouling propensity in reverse electrodialysis operated with hypersaline brine. *Energy* **2021**, *228*, 120563.

(4) Rijnaarts, T.; Moreno, J.; Saakes, W.; Vosb, V.M.; Nijmeijer, K. Role of anion exchange membrane fouling in reverse electrodialysis using natural feed waters. *Colloid. Surf. A* **2019**, *560*, 198-204.

(5) Vermaas, D.A.; Kunteng, D.; Saakes, M.; Nijmeijer, K. Fouling in reverse electrodialysis under natural conditions. *Water Res.* **2013**, *47*, 1289-1298.

(6) Kotoka, F.; Merino-Garcia, I.; Velizarov, S. Surface modifications of anion exchange membranes for an improved reverse electrodialysis process performance: A review. *Membranes* **2020**, *10*, 160.

(7) Alabi, A.; AlHajaj, A.; Cseri, L.; Szekely, G.; Budd, P.; Zou, L. Review of nanomaterials-assisted ion exchange membranes for electromembrane desalination. *Nature Partner Journals Clean Water* **2018**, *1*, 10.

(8) Cuiming, W.; Tongwen, X.; Weihua, Y. Fundamental studies of a new hybrid (inorganic-organic) positively charged membrane: membrane preparation and characterizations. *J. Membr. Sci.* **2003**, *216*, 269-278.

Published by ACS Sustainable Chemistry and Engineering,
https://doi.org/10.1021/acssuschemeng.3c06320

(9) Zhao, Y.; Tang, K.; Liu, H.; Van der Bruggen, B.; Sotto Díaz, A.; Shen, J. Gao, C. An anion exchange membrane modified by alternate electro-deposition layers with enhanced monovalent selectivity. *J. Memb. Sci.* **2016**, *520*, 262-271.

(10) Ahmad, M.; Tang, C.; Yang, L.; Yaroshchuk, A.; Brueninga, M.L. Layer-by-layer modification of aliphatic polyamide anion-exchange membranes to increase Cl^{-}/SO_4^{2-} selectivity. *J. Memb. Sci.* **2019**, *578*, 209-219.

(11) Rijnaarts, T.; Reurink, D.M.; Radmanesh, F.; Vos, W.M.; Nijmeijer, K. Layer-by-layer coatings on ion exchange membranes: Effect of multilayer charge and hydration on monovalent ion selectivities. *J. Memb. Sci.* **2019**, *570-571*, 513-521.

(12) You, S.J.; Semblante, G.U.; Lu, S.C.; Damodar, R.A.; Wei, T.C. Evaluation of the antifouling and photocatalytic properties of poly(vinylidene fluoride) plasma-grafted poly(acrylic acid) membrane with self-assembled TiO_2. *J. Hard. Mater.* **2012**, *237-238*, 10-19.

(13) Sprick, C.G. Functionalization of silver nanoparticles on membranes and its influence on biofouling. MSc. Thesis, University of Kentucky, **2017**.

(14) Li, J.-H.; Shao, X.-S.; Zhou, Q.; Li, M.-Z.; Zhang, Q.-Q. The double effects of silver nanoparticles on the PVDF membrane: surface hydrophilicity and antifouling performance. *Appl. Surf. Sci.* **2013**, *26*, 663-670.

(15) Hao, L.; Liao, J.; Jiang, Y.; Zhu, J.; Li, J.; Zhao, Y.; Bruggen, V.B.; Sotto, A.; Shen, J. "Sandwich"-like structure modified anion exchange membrane with enhanced monovalent selectivity and fouling resistant. *J. Membr. Sci.* **2018**, *556*, 98-106.

(16) Jiang, S.; Wang, F.; Cao, X.; Slater, B.; Wang, R.; Sun, H.; Wang, H.; Shen, X.; Yao, Z. Novel application of ion exchange membranes for preparing effective silver and copper based antibacterial membranes. *Chemosphere* **2022**, *287*, 132131.

Published by ACS Sustainable Chemistry and Engineering,
https://doi.org/10.1021/acssuschemeng.3c06320

(17) Vaselbehagh, M.; Karkhanechi, H.; Mulyati, S.; Takagi, R.; Matsuyama, H. Biofouling phenomena on anion exchange membranes under the reverse electrodialysis process. *J. Memb. Sci.* **2017**, *530*, 232-239.

(18) Radzig, M.A.; Nadtochenko, V.A.; Koksharova, O.A.; Kiwi, J.; Lipasova, V.A.; Khmel, I.A. Antibacterial effects of silver nanoparticles on gram-negative bacteria: Influence on the growth and biofilms formation, mechanisms of action. *Colloids Surf. B.* **2013**, *102*, 300-306.

(19) Vaselbehagh, M.; Karkhanechi, H.; Mulyati, S.; Takagi, R.; Matsuyama, H. Improved antifouling of anion-exchange membrane by polydopamine coating in electrodialysis process. *Desalination* **2014**, *332*, 126-133.

(20) Gao, H.; Zhang, B.; Tong, X.; Chen, Y. Monovalent-anion selective and antifouling polyelectrolytes multilayer anion exchange membrane for reverse electrodialysis. *J. Memb. Sci.* **2018**, *567*, 68-75.

(21) Eti, M.; Cihanoğlu, A.; Güler, E.; Gomez-Coma, L.; Altıok, E.; Arda, M.; Ortiz, I.; Kabay, N. Further development of polyepichlorohydrin based anion exchange membranes for reverse electrodialysis by tuning cast solution properties. *Membranes* **2022**, *12*,1192.

(22) Qin, Y.; Ji, X.; Jing, J.; Liu, H.; Wu, H.; Yang, W. Size control over spherical silver nanoparticles by ascorbic acid reduction. *Colloids and Surfaces A: Physicochem. Eng. Aspects* **2010**, *372*, 172-176.

(23) Cihanoğlu, A.; Altınkaya, S. A facile route to the preparation of antibacterial polysulfone-sulfonated polyethersulfone ultrafiltration membranes using a cationic surfactant cetyltrimethylammonium bromide. *J. Membr. Sci.* **2020**, *594*, 117438.

(24) Steinigeweg, D.; Schlücker, S. Monodispersity and size control in the synthesis of 20-100 nm quasi-spherical silver nanoparticles by citrate and ascorbic acid reduction in glycerol-water mixtures. *Chem. Commun.* **2012**, *48*, 8682-8684.

Published by ACS Sustainable Chemistry and Engineering,
https://doi.org/10.1021/acssuschemeng.3c06320

(25) Agnihotri, S.; Mukherji, S.; Mukherji, S. Size-controlled silver nanoparticles synthesized over the range 5-100 nm using the same protocol and their antibacterial efficacy. *RSC Adv.* **2014**, *4*, 3974-3983.

(26) Mikac, L.; Ivanda, M.; Gotic, M.; Mihelj, T.; Horvat, L. Synthesis and characterization of silver colloidal nanoparticles with different coatings for SERS application. *J Nanopart Res* **2014**, *16*, 2748.

(27) Kamali, M.; Ghorashi, A.A.S.; Asadollahi, M.A. Controllable synthesis of silver nanoparticles using citrate as complexing agent: characterization of nanoparticles and effect of pH on size and crystallinity. *Iran. J. Chem. Chem. Eng* **2012**, *31*, *4*, 221-228.

(28) Rashid, M.U.; Bhuiyan, K.H.; Quayum, M.E. Synthesis of silver nano particles (Ag-NPs) and their uses for quantitative analysis of vitamin C tablets. *Dhaka Univ. J. Pharm. Sci.* **2013**, *12(1)*, 29-33.

(29) Zhu, X.; Bai, R.; Wee, K.H.; Liu, C.; Tang, S.L. Membrane surfaces immobilized with ionic or reduced silver and their anti-biofouling performances. *J Memb. Sci.* **2010**, *363*, 278-286.

(30) Li, W.; Xie, X.; Shi, Q.; Zeng, H.; OU-Yan, Y.; Chen, Y. Antibacterial activity and mechanism of silver nanoparticles on *Escherichia coli*. *Appl Microbiol Biotechnol* **2010**, *85*, 1115-1122.

(31) Vaselbehagh, M.; Karkhanechi, H.; Takagi, R.; Matsuyama, H. Biofouling phenomena on anion exchange membranes under the reverse electrodialysis process. *J. Membr. Sci.* **2017**, *530*, 232-239.

(32) Yuksel, M.; Tas, B.; Imer D.Y.; Koyuncu, I. Effect of silver nanoparticle (AgNP) location in nanocomposite membrane matrix fabricated with different polymer type on antibacterial mechanism. *Desalination* **2014**, *347*, 120-130.

Published by ACS Sustainable Chemistry and Engineering,
https://doi.org/10.1021/acssuschemeng.3c06320

(33) Radzig, M.A.; Nadtochenko, V.A.; Koksharova, O.A.; Kiwi, J.; Lipasova, V.A.; Khmela, I.A. Antibacterial effects of silver nanoparticles on gram-negative bacteria: influence on the growth and biofilms formation, mechanisms of action. *Colloids and Surfaces B: Biointerfaces* **2013**, *102*, 300-306.

(34) Karakoç, E.; Güler, E. Comparison of physicochemical properties of two types of polyepichlorohydrin-based anion exchange membranes for reverse electrodialysis. *Membranes* **2022**, *12*, 257.

Published by ACS Sustainable Chemistry and Engineering,
https://doi.org/10.1021/acssuschemeng.3c06320

For Table of Contents Use Only

Silver nanoparticles (AgNPs) successfully coated onto the anion exchange membrane surface have increased both antibacterial activity and power density.

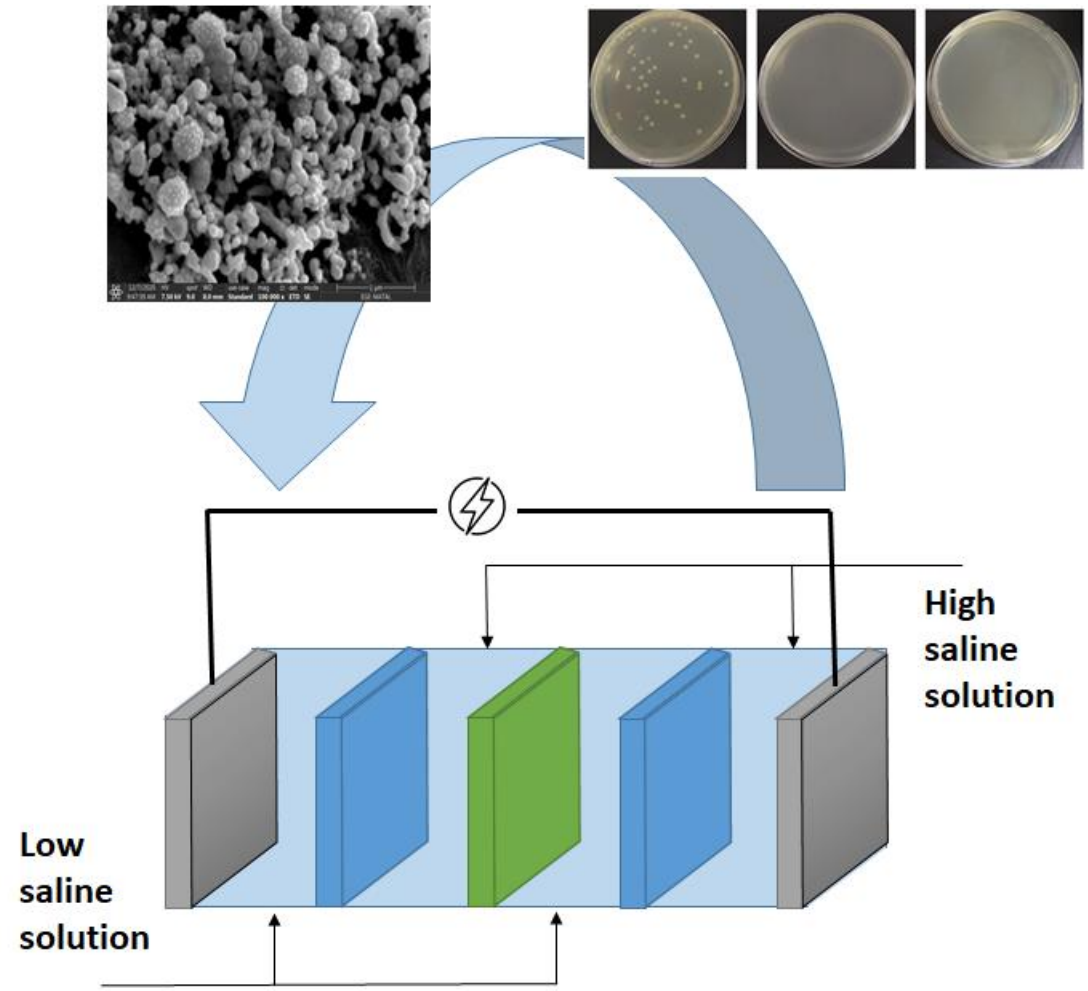

Published by ACS Sustainable Chemistry and Engineering,
https://doi.org/10.1021/acssuschemeng.3c06320